J. Biomechanics Vol. 22, No. 3, pp. 189–199, 1989.
Printed in Great Britain

0021 9290/89 $3.00 + .00
Pergamon Press plc

AN APPLICATION OF BEAM THEORY TO DETERMINE THE STRESS AND DEFORMATION OF LONG BONES

ERIC PAUL SALATHE, JR
Eastern Scientific and Education Foundation, 32 North West Street, Allentown, PA 18102, U.S.A.

GEORGE A. ARANGIO
Eastern Scientific and Education Foundation, and Lehigh Valley Hospital Center, Allentown, PA 18103, U.S.A.

and

ERIC P. SALATHE
Department of Mathematics, Lehigh University, Bethlehem, PA 18015, U.S.A.

Abstract—We present a generalized beam theory in which deformation and load are determined simultaneously, in order to analyze statically indeterminant problems involving long bones. We regard a long bone as a beam curved in three dimensions for which the cross-sectional properties vary continuously along its length. The theory is used to determine the force, moment, deflection and twist along the fifth metatarsal when it is subjected to both a pointwise and a distributed load.

INTRODUCTION

The idea of analyzing the stresses in long bones using beam theory is a fairly obvious one and can be traced at least as far back as 1917, when the *American Journal of Anatomy* published a comprehensive study of the femur by Koch (1917), in which he discussed basic principles of engineering mechanics and gave a careful review of beam theory. Regarding the femur as a curved beam in two dimensions, he traced out an approximate neutral axis on the bone, sliced it into 75 cross-sections perpendicular to this axis and computed the area and principle moments of inertia for each section. The resultant force and moment along the bone were determined from the applied external loads using simple considerations of static equilibrium, and the distribution of these loads through the cross-section were found from standard techniques using the area and moments of inertia at that section. Koch discussed various physiological and anatomical features of the bone in the light of his results. His analysis has been frequently repeated, applied to other bones and extended to represent the bone as curved in three dimensions (Cowin *et al.*, 1985; Huiskes, 1982; Rybicki *et al.*, 1972; Torodis, 1969).

Although most investigators now use finite element techniques to determine the stresses within bones, and these analyses have generally supported the appropriateness of simple beam theory (Rybicki *et al.*, 1972; Valliappan *et al.*, 1977), the ideas introduced by Koch have never been developed to the point where the full power of beam theory can be brought to bear on problems of orthopedic biomechanics. The simple statically determinate problems that were the focus of past studies permit immediate computation of the resulting force and moment at any cross-section through considerations of equilibrium, and the distributions of stress within the cross-section are then calculated by standard means. However, most of the problems occurring in orthopedic biomechanics are statically indeterminant. Generally a bone is held at its ends by ligaments and the forces exerted by these ligaments are affected by the deformation of the bone. A bone cantilevered at one end, or supported by pin-joints at each end, and therefore presenting a simple statically determinant problem, is not a biomechanically realistic situation. Even more interesting uses for beam theory are offered by the system consisting of the radius, ulna and humerus or the tibia, fibula and femur. In the latter case, for example, the load is transmitted by the femur onto the tibia and fibula in a complex manner that can only be determined by the simultaneous consideration of the loading and distortion of all three bones. The rib cage is a complex statically indeterminate structure composed of many long bones, each affected by the load placed on every one of the others. A further example is presented by the fifth metatarsal, which because of its anatomical disposition, is subjected to a distributed load along its length. This distributed load is affected by the deformation of the bone, and an interesting statically indeterminant problem in beam theory results.

In this paper we present a general theory of beams, in which the deformation and load are simultaneously considered, in a manner suitable for application to long bones. The bone is regarded as a beam curved in three dimensions for which the cross-sectional

Received in final form 20 *October* 1987.

properties vary continuously along its length. As originally noted by Koch, the cross-sectional properties in the plane taken perpendicular to the centroidal axis are required for the theory. Clearly, the centroidal axis cannot be determined until the bone is cross-sectioned, so as a practical matter we develop the theory in terms of data that can be collected from a series of parallel cross-sections taken perpendicular to a fixed axis oriented along the general direction of the bone. We illustrate the use of our theory by obtaining appropriate data for the fifth metatarsal and calculating the load and deformation along the length of the bone when it is subjected to both a pointwise and a distributed load.

THE GOVERNING EQUATIONS

The centroidal axis of the bone is a three-dimensional curve, defined in the fixed coordinate system (x, y, z) by $x=\bar{x}(s)$, $y=\bar{y}(s)$, $z=\bar{z}(s)$, where s is arc length. At each location s along the curve we define a local coordinate system $[x'(s), y'(s), z'(s)]$ by the orthogonal transformation

$$\begin{pmatrix} x'(s) \\ y'(s) \\ z'(s) \end{pmatrix} = \mathbf{C}(s) \left\{ \begin{pmatrix} x \\ y \\ z \end{pmatrix} - \begin{pmatrix} \bar{x}(s) \\ \bar{y}(s) \\ \bar{z}(s) \end{pmatrix} \right\},$$

as illustrated in Fig. 1. This transformation is chosen so that the z' axis is tangent to the centroidal axis at the location s and x', y' are the principle axes of the cross-section perpendicular to the centroidal axis. If $\mathbf{i}$, $\mathbf{j}$, $\mathbf{k}$ are the unit vectors along the fixed (x, y, z) axes, and if $\mathbf{i}'(s)$, $\mathbf{j}'(s)$, $\mathbf{k}'(s)$ are the unit vectors along the local coordinate axes $[x'(s), y'(s), z'(s)]$, then

$$\mathbf{C} = \begin{pmatrix} \mathbf{i}\cdot i' & \mathbf{j}\cdot i' & \mathbf{k}\cdot i' \\ \mathbf{i}\cdot j' & \mathbf{j}\cdot j' & \mathbf{k}\cdot j' \\ \mathbf{i}\cdot k' & \mathbf{j}\cdot k' & \mathbf{k}\cdot k' \end{pmatrix}.$$

At each location s, the internal forces exerted across a surface normal to the centroidal axis by that portion of the bone corresponding to lesser values of s upon that portion of the bone corresponding to greater values of s are equivalent to a force $\mathbf{F}(s)$ through the centroid and a moment $\mathbf{M}(s)$. Under the action of applied loads, the centroidal axis at location s undergoes a displacement $\mathbf{D}(s)$, and the local coordinate system there undergoes a rotation $\mathbf{T}(s)$. We shall derive a system of 12 coupled differential equations for the components of these four vectors referred to the fixed axes (x, y, z).

Figure 2 shows the portion of the bone between s and $(s+\Delta s)$. Because the bone is only slightly curved and its cross-sectional area varies slowly, this small element may be regarded as a cylinder with axis $z'(s)$ and ends perpendicular to its generators. The equations relating the forces and deformation for such an element can be readily derived when referred to the principle axes $x'(s)$, $y'(s)$, $z'(s)$ (see, for example, Timoshenko and Young, 1945). Forces $\mathbf{F}(s)$ and $-\mathbf{F}(s+\Delta s)$ act on the end surfaces and a distributed load acts on the cylindrical surface as a result of the interaction between the bone and its environment. This distributed load is equivalent to a force $\mathbf{P}^*(s, \Delta s)$ acting through the centroid of the volume element and a moment $\mathbf{Q}^*(s, \Delta s)$. We define the distributed load per unit length, $\mathbf{P}(s)$, and the distributed moment per unit length, $\mathbf{Q}(s)$, by

$$\mathbf{P}(s) = \lim_{\Delta s \to 0} \frac{\mathbf{P}^*(s, \Delta s)}{\Delta s}, \quad \mathbf{Q}(s) = \lim_{\Delta s \to 0} \frac{\mathbf{Q}^*(s, \Delta s)}{\Delta s}.$$

From a balance of the forces acting on the volume element, we obtain

$$\frac{d\mathbf{F}}{ds} = \mathbf{P}(s). \tag{1}$$

A balance of the moments about the centroidal axis at the location s yields

$$\begin{aligned} &\mathbf{M}(s) - \mathbf{M}(s+\Delta s) + \mathbf{Q}^*(s, \Delta s) \\ &\quad + (\Delta s/2)\mathbf{k}' \times \mathbf{P}^*(s, \Delta s) \\ &\quad - \Delta s\, \mathbf{k}' \times \mathbf{F}(s+\Delta s) = 0. \end{aligned}$$

In the limit $\Delta s \to 0$, this gives

$$\frac{d\mathbf{M}}{ds} = -\mathbf{k}' \times \mathbf{F} + \mathbf{Q}. \tag{2}$$

We note that $\mathbf{Q}$ must be a vector of the form $\mathbf{Q} = |\mathbf{Q}|k'$, and that for frictionless distributed load $\mathbf{P}\cdot\mathbf{k}' = 0$.

The displacement $\mathbf{D}(s+\Delta s)$ at the point $(s+\Delta s)$ along the centroidal axis differs from the displacement $\mathbf{D}(s)$ at the point s because of the change in the distance between s and $s+\Delta s$ and because of a rota-

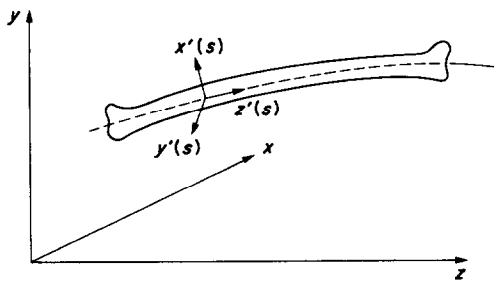

Fig. 1. The local coordinate system.

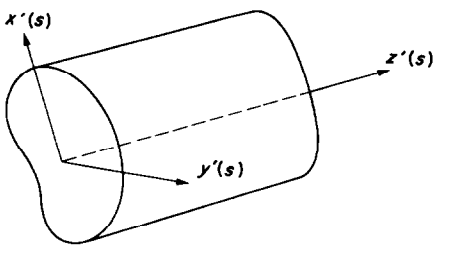

Fig. 2. The portion of the bone between s and $(s+\Delta s)$.

tion $\mathbf{T}(s)$ in the local coordinate system at s. Therefore

$$\frac{d\mathbf{D}}{ds} = -\frac{1}{EA'(s)}(\mathbf{k}'\cdot\mathbf{F})\mathbf{k}' - \mathbf{k}'\times\mathbf{T}, \tag{3}$$

where E is Young's modulus and A' is the cross-sectional area.

The components, referred to the local coordinate system, of the forces and moments acting on the end surfaces of the element between s and $(s+\Delta s)$ are illustrated in Fig. 3. The y' component of the force $\mathbf{F}$ at $(s+\Delta s)$ causes a difference in the y' component of the displacement at s and $s+\Delta s$ given by $D_{y'}(s)-D_{y'}(s+\Delta s)=F_{y'}(s+\Delta s)(k_{x'}/A'G)\Delta s$ where $k_{x'}$ is a factor depending on the shape of the cross-section at s and G is the shear modulus. Using $dD_{y'}/ds=-T_{x'}$, derived earlier, adding the effect of the moments, and recalling equation (1), we obtain

$$\frac{dT_{x'}}{ds} = -\frac{1}{EI_{x'x'}}M_{x'} + \frac{k_{x'}}{A'G}P_{y'}. \tag{4}$$

It follows in a completely analogous manner that

$$\frac{dR_{y'}}{ds} = -\frac{1}{EI_{y'y'}}M_{y'} - \frac{k_{y'}}{A'G}P_{x'}, \tag{5}$$

where $k_{y'}$ is also a factor depending on the shape of the cross-section, and $I_{x'x'}$, $I_{y'y'}$ are the principle moments of inertia.

The segment from s to $(s+\Delta s)$ twists about the z' axis because of the moment $M_{z'}$ and because the force $\mathbf{F}$ acts through the centroid and not through the shear center of the cross-section. If $x_c'(s)$, $y_c'(s)$ are the local coordinates of the shear center then

$$\frac{dT_{z'}}{ds} = \frac{1}{K'G}\{-M_{z'} - F_{y'}x_c' + F_{x'}y_c'\} \tag{6}$$

where K' depends on the cross-section shape and $K'G$ is the torsional rigidity.

Defining the 12-vector

$$\Phi' = (F_{x'}, F_{y'}, F_{z'}, M_{x'}, M_{y'}, M_{z'}, D_{x'}, D_{y'}, D_{z'}, T_{x'}, T_{y'}, T_{z'})^T, \tag{7}$$

where the superscript T denotes transpose, the governing equations (1–6) can be written in matrix form as

$$\frac{d}{ds}\Phi_i' = A_{ij}'\Phi_j' + B_i'. \tag{8}$$

A_{ij}' are the components of a 12×12 matrix $\mathbf{A}$, given by

$$\mathbf{A}' = \begin{bmatrix}
0 & 0 & 0 & 0 & 0 & 0 & 0 & 0 & 0 & 0 & 0 & 0 \\
0 & 0 & 0 & 0 & 0 & 0 & 0 & 0 & 0 & 0 & 0 & 0 \\
0 & 0 & 0 & 0 & 0 & 0 & 0 & 0 & 0 & 0 & 0 & 0 \\
0 & 1 & 0 & 0 & 0 & 0 & 0 & 0 & 0 & 0 & 0 & 0 \\
-1 & 0 & 0 & 0 & 0 & 0 & 0 & 0 & 0 & 0 & 0 & 0 \\
0 & 0 & 0 & 0 & 0 & 0 & 0 & 0 & 0 & 0 & 0 & 0 \\
0 & 0 & 0 & 0 & 0 & 0 & 0 & 0 & 0 & 0 & 1 & 0 \\
0 & 0 & 0 & 0 & 0 & 0 & 0 & 0 & 0 & -1 & 0 & 0 \\
0 & 0 & \frac{-1}{EA'} & 0 & 0 & 0 & 0 & 0 & 0 & 0 & 0 & 0 \\
0 & 0 & 0 & \frac{-1}{EI_{x'x'}} & 0 & 0 & 0 & 0 & 0 & 0 & 0 & 0 \\
0 & 0 & 0 & 0 & \frac{-1}{EI_{y'y'}} & 0 & 0 & 0 & 0 & 0 & 0 & 0 \\
\frac{y_c'}{K'G} & \frac{-x_c'}{K'G} & 0 & 0 & 0 & \frac{-1}{K'G} & 0 & 0 & 0 & 0 & 0 & 0
\end{bmatrix} \tag{9}$$

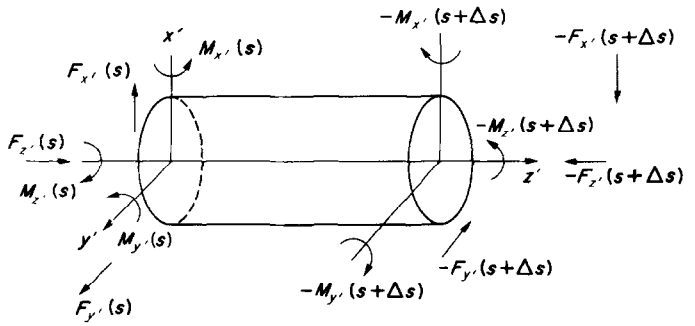

Fig. 3. The components, referred to the local coordinate system, of the forces and moments acting on the element between s and $(s+\Delta s)$.

and B'_i are the components of the vector $\mathbf{B}'$ given by

$$\mathbf{B}'=\left(P_{x'}, P_{y'}, 0, 0, 0, Q_{z'}, 0, 0, 0, \frac{k_{x'}}{A'G}P_{y'}, -\frac{k_{y'}}{A'G}P_{x'}, 0\right)^T. \quad (10)$$

We have assumed here that $\mathbf{P}$ and $\mathbf{Q}$ are known functions, independent of Φ'. We will discuss in a later section the modifications that are necessary when they depend on the deflection of the bone.

Equation (8) applies to the small cylindrical element between s and $(s+\Delta s)$ and was derived for the components of $\mathbf{F}$, $\mathbf{M}$, $\mathbf{D}$ and $\mathbf{T}$ referred to the local coordinate system (x', y', z') at s. It cannot be regarded as a global equation valid for all s unless it is rewritten in terms of the components referred to the fixed coordinate system (x, y, z). Defining the vector Φ by

$$\Phi=(F_x, F_y, F_z, M_x, M_y, M_z, D_x, D_y, D_z, T_x, T_y, T_z), \quad (11)$$

and the matrix $\mathbf{N}$ by

$$\mathbf{N}=\begin{bmatrix}\mathbf{C} & \mathbf{0} & \mathbf{0} & \mathbf{0}\\ \mathbf{0} & \mathbf{C} & \mathbf{0} & \mathbf{0}\\ \mathbf{0} & \mathbf{0} & \mathbf{C} & \mathbf{0}\\ \mathbf{0} & \mathbf{0} & \mathbf{0} & \mathbf{C}\end{bmatrix}, \quad (12)$$

where $\mathbf{0}$ denotes a 3×3 zero matrix, it follows that

$$\Phi'_i=N_{ij}\Phi_j. \quad (13)$$

Equation (8) can then be put into the form

$$\frac{\mathrm{d}}{\mathrm{d}z}\Phi=\mathbf{A}\Phi+\mathbf{B}, \quad (14)$$

where $\mathbf{A}=(\mathbf{N}^{-1}\mathbf{A}'\mathbf{N})\cdot\sec\phi$, $\mathbf{B}=(\mathbf{N}^{-1}\mathbf{B}')\sec\phi$, and $\phi(s)$ is the angle between the centroidal axis and the fixed z-axis. Removing $\mathbf{N}$ from inside the derivative is justified, since for the small cylindrical element the (x', y', z') coordinate system is fixed and s is distance along the z' axis. However, in the present form, equation (14) can be regarded as a global equation for Φ, applicable all along the bone, with $\mathbf{A}$ and $\mathbf{B}$ known functions of s. To complete these equations it is necessary to determine the matrices $\mathbf{A}'$ and $\mathbf{C}$ (and therefore the matrix $\mathbf{A}$) as a function of distance along the bone.

THE LOCAL COORDINATE SYSTEM AND THE CROSS-SECTION PROPERTIES

The local coordinate system is chosen with the z' axis along the centroidal axis of the bone and the x' and y' axes along the principle axes in a cross-section normal to the centroidal axis. To determine this coordinate system and the principal moments of inertia, the area, and the other cross-sectional properties in the (x', y') plane, the bone is placed in a mold in such a way that it is generally aligned with the fixed z-axis, as shown in Fig. 4, and the mold is filled with a

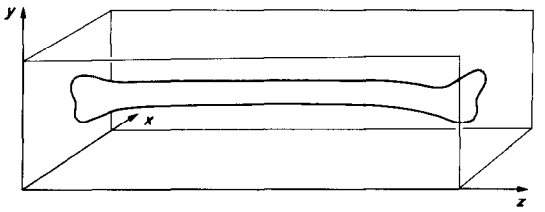

Fig. 4. The bone in a clear plastic mold, defining the fixed coordinate system (x, y, z).

clear resin mixed with hardener. After the mixture hardens, numerous slices are taken perpendicular to the z-axis, and for each slice the cross-section of the bone, together with the fixed x and y axes, are photographed and enlarged, as shown in Fig. 5. The cross-sectional shapes are transferred to the computer using a digitizer and we compute, for each location z at which a cut is made, the coordinates $(x_c(z), y_c(z))$ of the centroidal axis, the area A, and the moments and product of inertia, I_{xx}, I_{yy}, I_{xy}, relative to the fixed x–y axes. The values of these quantities, determined for a discrete set of z, are fitted to a sum of Legendre Polynomials using the method of least squares. (Legendre Polynomials are chosen because their orthogonality property facilitates the use of the least squares method by generating a nearly diagonal matrix in the equation for the coefficients.) Therefore, each of these quantities may be regarded as a given analytic function of z.

The unit vector in the direction of the centroidal axis, k', is

$$k'=\frac{\frac{\mathrm{d}x_c}{\mathrm{d}z}\mathbf{i}+\frac{\mathrm{d}y_c}{\mathrm{d}z}\mathbf{j}+\mathbf{k}}{\sqrt{\left(\frac{\mathrm{d}x_c}{\mathrm{d}z}\right)^2+\left(\frac{\mathrm{d}y_c}{\mathrm{d}z}\right)^2+1}}. \quad (15)$$

The cross-section of the bone perpendicular to the centroidal axis is obtained by rotating the cross-section perpendicular to the fixed z-axis through an angle $\theta=\cos^{-1}(\mathbf{k}\cdot\mathbf{k}')$ about the axis $\mathbf{i}^*=(\mathbf{k}\times\mathbf{k}')/|\mathbf{k}\times\mathbf{k}'|$, as shown in Fig. 6. The axes $\mathbf{i}^*$ and $\mathbf{j}^*=\mathbf{k}'\times\mathbf{i}^*$ lie in the plane perpendicular to the centroidal axis, but they are not the principle axes. They do, however, provide reference axes, relative to which the principle axes can be defined. The axes $\hat{\mathbf{i}}=\mathbf{i}^*$, $\hat{\mathbf{j}}=\mathbf{k}\times\mathbf{i}^*$ lie in the plane perpendicular to the z-axis. The moments and product of inertia relative to these axes are

$$\begin{aligned}I_{\hat{x}\hat{x}}&=(\hat{\mathbf{j}}\cdot\mathbf{j})^2(I_{xx}-y_c^2A)\\&\quad+2(\hat{\mathbf{j}}\cdot\mathbf{j})(\hat{\mathbf{j}}\cdot\mathbf{i})(I_{xy}-x_cy_cA)\\&\quad+(\hat{\mathbf{j}}\cdot\mathbf{i})^2(I_{yy}-x_c^2A)\\I_{\hat{y}\hat{y}}&=(\hat{\mathbf{i}}\cdot\mathbf{j})^2(I_{xx}-y_c^2A)\\&\quad+2(\hat{\mathbf{i}}\cdot\mathbf{i})(\hat{\mathbf{i}}\cdot\mathbf{j})(I_{xy}-x_cy_cA)\\&\quad+(\hat{\mathbf{i}}\cdot\mathbf{i})^2(I_{yy}-x_c^2A)\\I_{\hat{x}\hat{y}}&=[(\hat{\mathbf{i}}\cdot\mathbf{i})(\hat{\mathbf{j}}\cdot\mathbf{j})+(\hat{\mathbf{i}}\cdot\mathbf{j})(\hat{\mathbf{j}}\cdot\mathbf{i})](I_{xy}-x_cy_cA)\\&\quad+(\hat{\mathbf{i}}\cdot\mathbf{j})(\hat{\mathbf{j}}\cdot\mathbf{j})(I_{xx}-y_c^2A)+(\hat{\mathbf{i}}\cdot\mathbf{i})(\hat{\mathbf{j}}\cdot\mathbf{i})(I_{yy}-x_c^2A).\end{aligned}$$

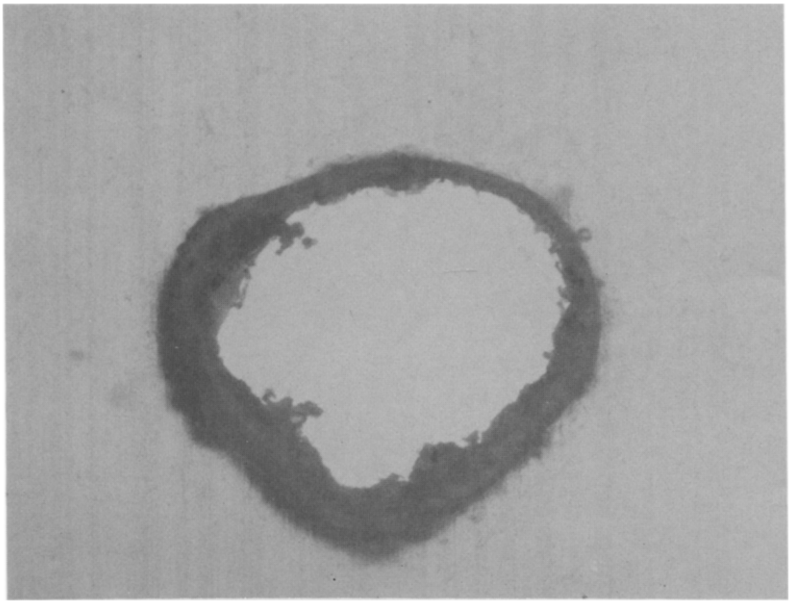

Fig. 5. A cross-section of the fifth metatarsal, taken perpendicular to the fixed z-axis.

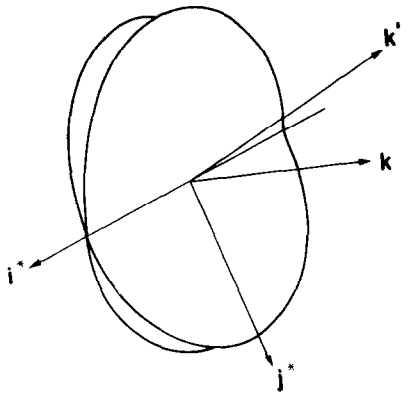

Fig. 6. The cross-sections perpendicular to the fixed z-axis and perpendicular to the centroidal axis $z'(s)$ at the location s.

The moments and products of inertia in the coordinate system defined by (i^*, j^*) in the plane perpendicular to the centroidal axis are

$$I_{x^*x^*} = \cos^3\theta\, I_{\hat{x}\hat{x}}$$
$$I_{x^*y^*} = \cos^2\theta\, I_{\hat{x}\hat{y}}$$
$$I_{y^*y^*} = \cos\theta\, I_{\hat{y}\hat{y}}.$$

The area of the bone in the cross-section perpendicular to the centroidal axis, A', and the area in the cross-section perpendicular to the fixed z-axis, A, are related by $A' = A\cos\theta$.

Principle axes are obtained by rotating the (x^*, y^*) axes through an angle

$$\phi^* = \frac{1}{2}\tan^{-1}\frac{2I_{x^*y^*}}{I_{y^*y^*} - I_{x^*x^*}}. \tag{16}$$

For any cross-section, there are four possible ways to choose the principle axes, and this definition always selects them so that the x' axis lies in the quadrant $-\pi/4 < \phi^* \leq \pi/4$; therefore it does not provide a continuously varying local coordinate system along the length of the bone. If we arbitrarily select the x' axis so that $I_{x'x'} < I_{y'y'}$, then for any shape there are only two possible choices for the angle through which the (x^*, y^*) coordinates may be rotated. These are denoted by ϕ_p and $\phi_n = \phi_p + \pi$ and are determined by the following scheme.

If $I_{x^*y^*} \geq 0$ and $I_{y^*y^*} \geq I_{x^*x^*}$

then $\phi_p = \phi^*$, $\phi_n = \phi^* + \pi$.

If $I_{x^*y^*} \geq 0$ and $I_{y^*y^*} < I_{x^*x^*}$

then $\phi_p = \phi^* + \pi/2$, $\phi_n = \phi^* + 3\pi/2$.

If $I_{x^*y^*} < 0$ and $I_{y^*y^*} \leq I_{x^*x^*}$

then $\phi_p = \phi^* + \pi/2$, $\phi_n = \phi^* + 3\pi/2$.

If $I_{x^*y^*} < 0$ and $I_{y^*y^*} > I_{x^*x^*}$

then $\phi_p = \phi^* + \pi$, $\phi_n = \phi^* + 2\pi$.

For the first cross-section we rotate the (x^*, y^*) axes through the angle $\phi = \phi_p$, and for each subsequent location we make the choice for ϕ between ϕ_p and ϕ_n that gives the smaller difference from the value at the previous location. This provides a continuously varying local coordinate system provided the cross-section does not assume a circular shape at any location. This scheme breaks down if ϕ changes from a small positive value ε at s to a small negative value $-\delta$ at $(s+\Delta s)$. The choices presented by the above scheme for ϕ at $(s+\Delta s)$ are then $\phi_p = \phi^* + \pi = \pi - \delta$ and $\phi_n = \phi^* + 2\pi = 2\pi - \delta$, and the incorrect value $\pi - \delta$ will be selected. This can be corrected by introducing an additional requirement that if the change in ϕ is not sufficiently small then we make the choice for ϕ between ϕ_p and ϕ_n that gives the larger difference from the value at the previous location. In practice, if the value for ϕ is printed out for each location z, then it can be verified that the local coordinate system does in fact vary continuously along the length of the bone.

The principle moments of inertia are given by

$$I_{x'x'} = I_{x^*x^*}\cos^2\phi + I_{y^*y^*}\sin^2\phi - I_{x^*y^*}\sin 2\phi, \tag{17}$$
$$I_{y'y'} = I_{y^*y^*}\sin^2\phi + I_{y^*y^*}\cos^2\phi + I_{x^*y^*}\sin 2\phi,$$

and the unit vectors in the direction of the principle axes are

$$\mathbf{i}' = \cos\phi\,\mathbf{i} + \sin\phi\,\mathbf{j}^* \tag{18}$$
$$\mathbf{j}' = \mathbf{k}' \times \mathbf{i}'. \tag{19}$$

Clearly, at each location z the principle axes (and therefore the matrix $\mathbf{C}$) and the area and principle moments of inertia appearing in matrix $\mathbf{A}'$ can be found through routine computation. (The shape factors and shear center locations in the matrix $\mathbf{A}'$ can be found in a similar manner. However, in the problems to be treated in this paper, we assumed for simplicity that $x_c' = y_c' = 0$, that the shape factors $k_{x'}$, $k_{y'}$ are equal to unity, and that $K' = I_p = I_{x'x'} + I_{y'y'}$.) The matrix $\mathbf{A}$ in equation (14) is therefore a known function of z. The right-hand side must be considered separately for each application, since it depends on the nature of the distributed load. This will be discussed further in the next section.

APPLICATION TO THE FIFTH METATARSAL

The six equations for the force and moment decouple from the six equations for the deflection and twist, as can be seen from the form of $\mathbf{A}'$. Therefore, for certain bones, such as the metatarsals where the forces and moments are known at the metatarsal head, a straightforward Runge–Kutta technique beginning at one end can be used for the first six equations. Beginning again at the other end, where boundary conditions for the deflection and twist are specified, and with the forces and moments now known, a

Runge–Kutta technique can then be applied to the second set of six equations. However, in general the force and moment cannot be determined independently of the deflection and twist because of the boundary conditions; application of beam theory to long bones generally leads to statically indeterminate problems, as pointed out in the introduction. At each end complex relationships between deflection, twist, force and moment exist, and we are led to a two point boundary value problem for the full set of 12 coupled equations. This is the case for the fifth metatarsal, which is of special interest since it is subject to the Jones' fracture (Arangio, 1983). Because of its orientation, a distributed load exists along the fifth metatarsal, transmitted from the ground up through the tissue that lies between it and the bone, as illustrated in Fig. 7. Since this distributed load is affected by the upward deflection of the metatarsal, it cannot be represented by the vector $\mathbf{B}'$ in equation (8); it contributes elements to the upper right quadrant of the matrix $\mathbf{A}'$. Equation (14) therefore remains coupled and the analysis of the fifth metatarsal presents a two-point boundary value problem for the 12 unknowns.

We assume that an upward force of magnitude F_A is applied in the fixed y direction at the metatarsal head, $z=L$, and that the metatarsal is rigidly fixed at its base, $z=0$. A relationship between the moment and the twist at $z=0$ would be more appropriate. However, not only does the metatarsal–cuneiform joint deform, but so do all the joints of the midfoot under the action of applied loads. Therefore, until the present analysis is incorporated into the overall study of the deformation of the foot (Salathe *et al.*, 1986), it is reasonable to regard the metatarsal as rigidly attached at its base. The distributed load is due to a compressible elastic medium occupying the region below the bone and above the level $y=H$, which represents the ground, as shown in Fig. 7. Moving this level up an amount Δ (equivalent to moving the foot down) compresses the medium and causes a distributed load along the metatarsal. Clearly, the magnitude of this distributed load is

$$F_C = k\frac{\Delta - \Phi_8(z)}{y_B(z) - H}, \tag{20}$$

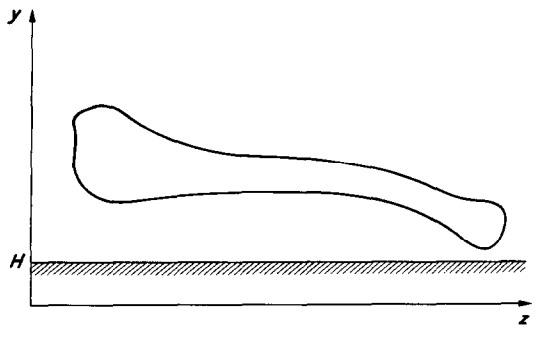

Fig. 7. The fifth metatarsal is subjected to a distributed load, transmitted by the ground located at $y=H$.

where the denominator gives the undeformed height of the material that is compressed and the numerator gives the extent of the compression. The constant k is a material constant and $y_B(z)$ is the y-component of the bottom of the bone in the cross-section at z. Since the distributed load must lie in the vertical plane containing the centroidal axis of the bone between s and $(s+\Delta s)$ and act perpendicular to the bone, it has the direction $\mathbf{k}'\times(\mathbf{j}\times\mathbf{k}')$. It can be shown that $\mathbf{j}\cdot[\mathbf{k}'\times(\mathbf{j}\times\mathbf{k}')]=1-(\mathbf{j}\cdot\mathbf{k}')\geq 0$, and so this is in the upward direction, as required. We assume that there is no applied moment associated with the distributed load, so that $Q_z=0$.

We can avoid a two-point boundary value problem for the fifth metatarsal by noting that since the bone is stiff a good first approximation to the distributed load can be obtained by neglecting the deflection, $\Phi_8(z)$, in equation (20). The distributed load is then known and can be represented by the vector $\mathbf{B}$; the form of equation (14) is unchanged. Therefore, as noted above, the first six equations can be solved with a Runge–Kutta technique beginning at the metatarsal head, and the second set can subsequently be solved in a similar way starting at the metatarsal base. With the deflections determined, a better approximation to the magnitude of the distributed load is found from equation (20), $\mathbf{B}$ in equation (14) is appropriately modified, and the above procedure is repeated until convergence occurs.

The equations derived for the rotation $\mathbf{T}$ include the effect of both bending moment and shear force. The contribution of the distributed load to the shear force appears explicitly in equations (4) and (5). For beams of constant cross-sectional shape, the concentrated loads are accounted for by specifying appropriate initial conditions on $\mathbf{T}$ at $z=0$. In the present case this would involve specifying $\Phi_{10}=-F_A/AG$ at $z=0$. Because of the form of the equations, this would alter Φ_{10} by the constant amount $-F_A/AG$ along the bone. In the present theory we allow A to be a slowly varying function of z, and so we cannot account for the concentrated load through an initial condition. However, to the order of approximation introduced, we can account for F_A simply by altering Φ_{10} by the variable amount $-F_A/A(z)G$. Since this alteration in $\mathbf{T}$ has a complex effect on $\mathbf{D}$, we use instead the following slightly modified scheme. At each step along the Runge–Kutta procedure, we alter Φ_{10} by an amount corresponding to the value of $-F_A/A(z)G$ at that location z. The next step forward then yields a value for the displacement corresponding to the correct amount of rotation.

The cross-section in Fig. 5 is one of 32 obtained for the fifth metatarsal and Fig. 8 shows a reconstruction of the bone from these cross-sections. The values of X_c, Y_c, $I_{xx}-y_c^2A$, $I_{yy}-X_c^2A$, $I_{xy}-X_cy_cA$, A and y_B were determined for each cross-section and are shown in Figs 9–15 at the values of z to which they correspond. The bone extends over the range $0\leq z\leq 5.004$ cm. The smooth curve in each figure is

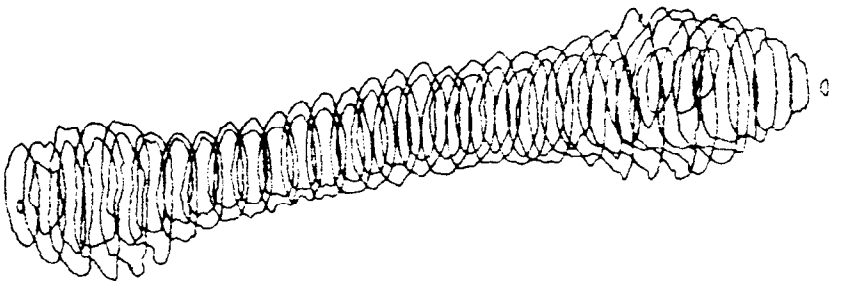

Fig. 8. A computer reconstruction of the fifth metatarsal from the data obtained at each cross-section. In this figure the base of the metatarsal ($z=0$) is at the right.

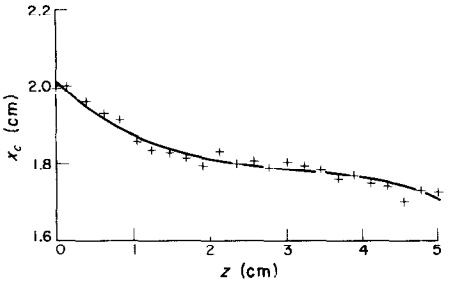

Fig. 9. The x-component of the centroidal axis, $x_c(z)$. The discrete points were determined for each cross-section, and the continuous curve is a least-squares fit to a series of four Legendre polynomials.

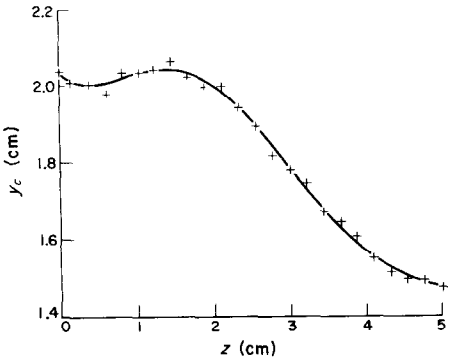

Fig. 10. The y-component of the centroidal axis, $y_c(z)$. The discrete points were determined for each cross-section, and the continuous curve is a least-squares fit to a series of six Legendre polynomials.

the result of a least-squares fit by a series of Legendre Polynomials. The number of such polynomials used to obtain the best fit for each variable is indicated in the figure caption. A separate program was written for the curve fitting, and the coefficients of the Legendre Polynomial expansion that give the curves shown in Figs 9–14 and the calculated bone length were used as input into the main program.

Other data needed for the numerical examples are Young's modulus for bone, $E=1.8\times10^6\ \mathrm{N\,cm^{-2}}$, the shear modulus $G=E/3$, the magnitude of the applied load F_A, and the constants that determine the magni-

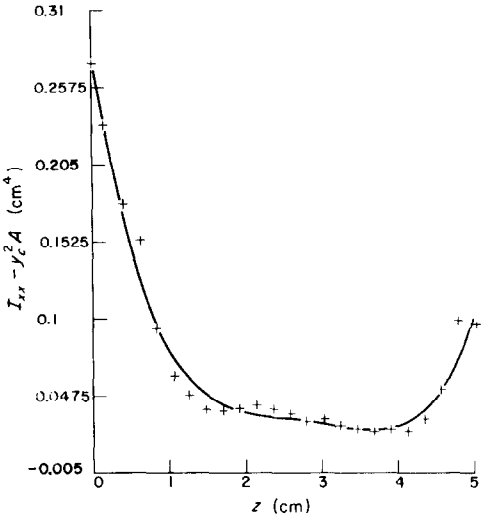

Fig. 11. The moment of inertia about an axis through the centroid parallel to the x-axis: $I_{xx}-y_c^2A$. The discrete points were determined from each cross-section, and the continuous curve is a least-squares fit to a series of five Legendre polynomials.

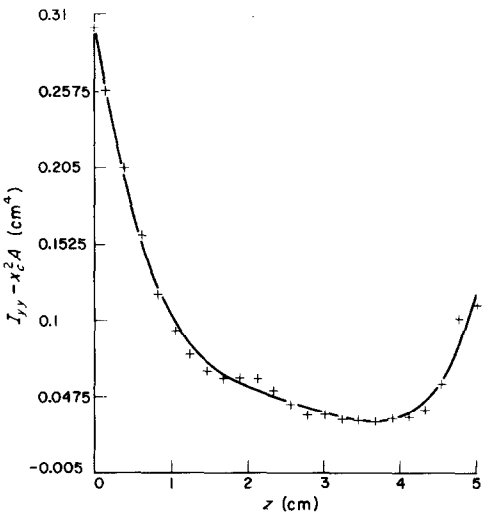

Fig. 12. The moment of inertia about an axis through the centroid parallel to the y-axis: $I_{yy}-x_c^2A$. The discrete points were determined for each cross-section, and the continuous curve is a least-squares fit to a series of six Legendre polynomials.

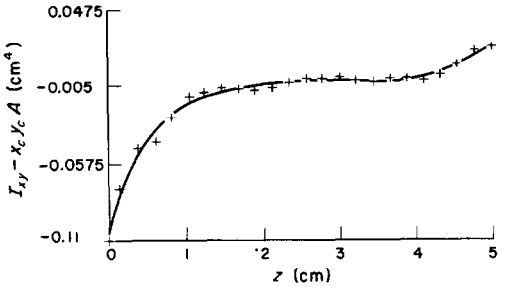

Fig. 13. The product of inertia relative to axes through the centroid parallel to the x–y axes: $I_{xy}-x_c y_c A$. The discrete points were determined for each cross-section, and the continuous curve is a least-squares fit to a series of eight Legendre polynomials.

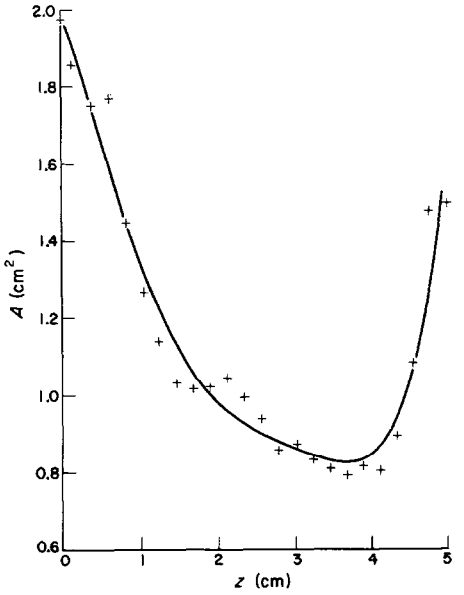

Fig. 14. The area A of the cross-section perpendicular to the fixed x-axis. The discrete points were determined for each cross-section, and the continuous curve is a least-squares fit to a series of six Legendre polynomials.

tude of the distributed load. We estimate these constants in the following way. By neglecting $\Phi_8(z)$ and specifying an estimated value, F_{TOT}, for the magnitude of the total distributed load along the length of the bone, it follows that

$$k=(F_{TOT}/\Delta)\left(\int_0^1 \frac{dz}{y_B(z)-H}\right)^{-1}. \qquad (21)$$

We selected values for H, F_{TOT}, and Δ, and calculated k from the above expression. These three quantities therefore uniquely specify the distributed load. Figures 16–19 show the three components of the force, moment, deflection and twist corresponding to $F_A=75$ N, $H=0.5$ cm and $\Delta=0.3$ cm. With $F_{TOT}=75$ N, we determine $k=35.8$ N cm^{-1}. Because of the upward deflection of the bone, this data

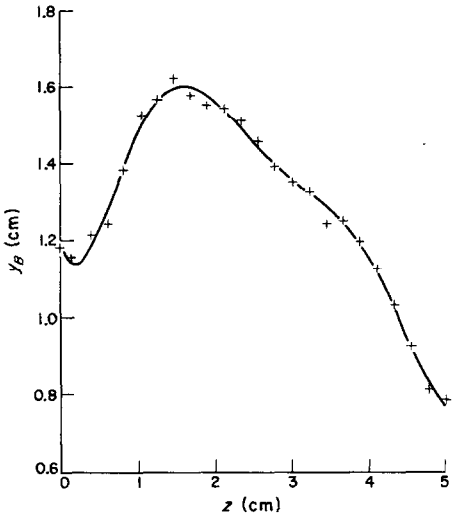

Fig. 15. The height of the bottom of the bone in any cross-section from the fixed x–z plane. The discrete points were determined for each cross-section, and the continuous curve is a least-squares fit to a series of seven Legendre polynomials.

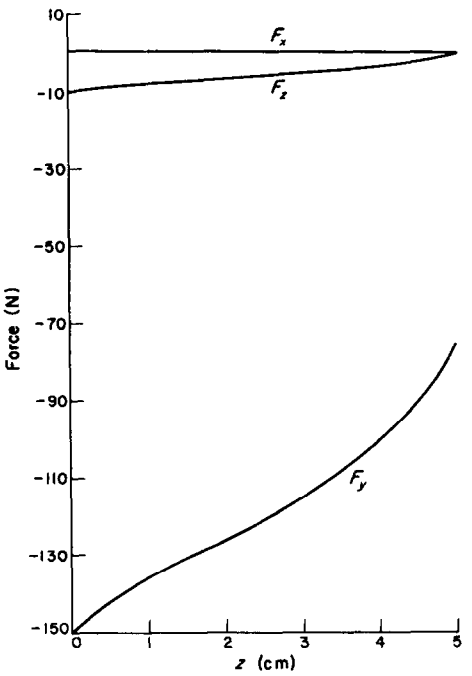

Fig. 16. The three components of the force along the length of the metatarsal.

corresponds to an actual total distributed load of 70.5 N along the length of the bone. Values of $\Delta=0.35$ cm and 0.25 cm give results that are very close to those shown in Figs 16–19. The choice $\Delta=0.25$ corresponds to a stiffer material with $k=43$ N cm^{-1} and the choice $\Delta=0.35$ corresponds to a more compliant material with $k=30.7$ N cm^{-1}. In the first case the actual total distributed load is 69.6 N,

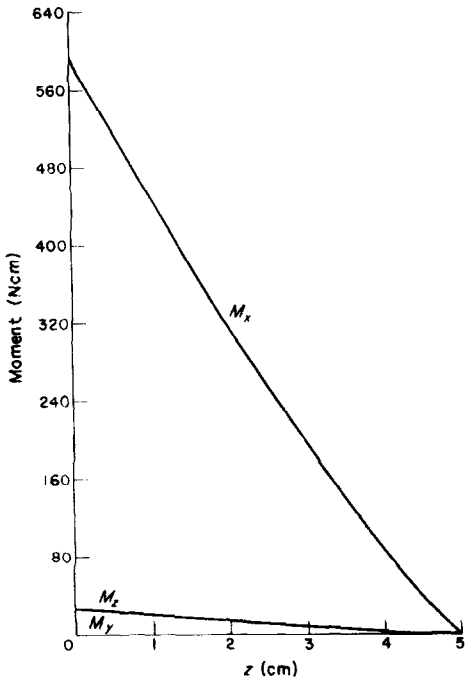

Fig. 17. The three components of the moment along the length of the metatarsal.

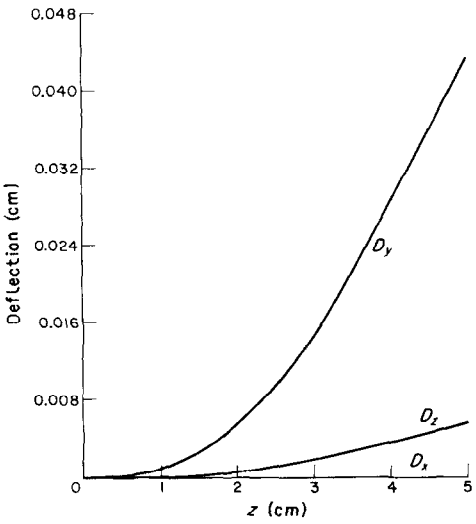

Fig. 18. The three components of the deflection along the length of the metatarsal.

and in the latter it is 71.1 N. Clearly, the solutions are not particularly sensitive to these parameters.

The theory presented here can be applied to a wide variety of statically indeterminant problems involving long bones to determine the force, moment, deflection and twist along the length of the bone. The distribution of stress throughout a cross-section can then be

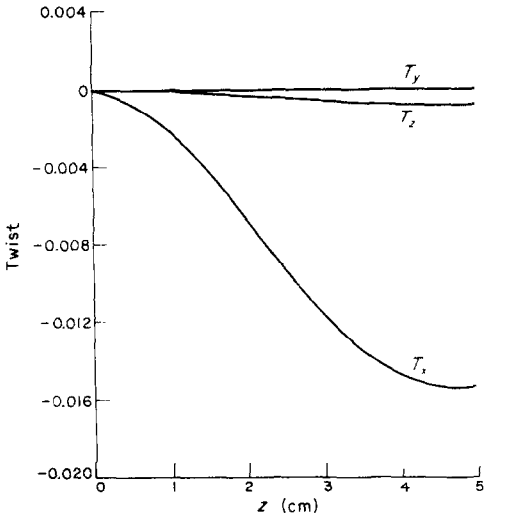

Fig. 19. The three components of the twist along the length of the metatarsal.

found using standard techniques. We have shown how the data required for the theory can be obtained through cross-sectioning of the bone and have carried out the procedure for the fifth metatarsal. Similar data can readily be obtained for any long bone of interest and an appropriate system of differential equations formulated and analyzed to determine the deformation and load in that bone.

Acknowledgements—The following Lehigh University students helped to cross-section the fifth metatarsal and obtain the data on the cross-sectional properties: Douglas Phillippy, Lisa Gravel, David Moharic and Lisa Ellis. This research was supported in part by a grant from the Pool Trust.

REFERENCES

Arangio, G. A. (1983) Proximal diaphyseal fractures of the fifth metatarsal (Jones' fracture): two cases treated by cross-pinning with review of 106 cases. *Foot and Ankle* **3,** 293–296.

Cowin, S. C., Hart, R. T. and Balser, J. R. (1985) Functional adaptation in long bones: establishing *in vivo* values for surface remodeling rate coefficients. *J. Biomechanics* **18,** 665–684.

Huiskes, R. (1982) On the modelling of long bones in structural analyses. *J. Biomechanics* **15,** 65–69.

Koch, J. C. (1917) The laws of the bone architecture. *Am. J. Anat.* **21,** 177–208.

Rybicki, E. F., Simonen, F. A. and Weis, Jr, E. F. (1972) On the mathematical analysis of stress in the human femur. *J. Biomechanics* **5,** 203–215.

Salathe, Jr, E. P., Arangio, G. A. and Salathe, E. P. (1986) A biomechanical model of the foot. *J. Biomechanics* **19,** 989–1001.

Timoshenko, S. and Young, D. H. (1945) *Theory of Structures.* McGraw Hill, New York.

Torodis, T. G. (1969) Stress analysis of the femur. *J. Biomechanics* **2,** 163–174.

Valliappan, S., Svensson, N. L. and Wood, R. D. (1977) Three-dimensional stress analysis of the human femur. *Comput. Biol. Med.* **7,** 253–264.